PbS quantum dot electroabsorption modulation across the extended communications band 1200–1700 nm

Ethan J. D. Klem,[a] Larissa Levina, and Edward H. Sargent
Department of Electrical and Computer Engineering, University of Toronto, Toronto, Ontario, M5S 3G4, Canada

(Received 10 November 2004; accepted 13 June 2005; published online 25 July 2005)

We report electric field-induced modulation of absorption in PbS nanocrystal quantum dots across the spectral region 600–2000 nm, encompassing the entire telecommunications band. The maxima in the electroabsorption spectra correspond with the positions of the first excitonic peak, confirming the predominance of excitonic broadening as the basis for the observed effect. We estimate the change in dipole moment to be on the order of 20 D in 7 nm diameter PbS nanocrystals compared to previously-reported ~100 D in CdSe. © *2005 American Institute of Physics*.
[DOI: 10.1063/1.2001737]

Semiconductor nanocrystals provide custom-tunable emission, modulation, and detection of light. To date, this full suite of functions has been demonstrated only in the visible spectral range; however, applications in data communication demand sources, detectors, and modulators in the extended telecommunications-wavelength band (1200–1700 nm).[1]

Extensive attention has recently been paid to achieving infrared electroluminescence from ZnSe(InAs),[2] PbS,[3] and PbSe[4] and infrared optical gain from PbSe.[5] However, there have to date been no demonstrations of electric-field-induced absorption modulation in the infrared from solution-processed quantum dots, critical to achieving controlled modulation of optical signals. Here we show the measurement of infrared electroabsorption in solution-synthesized quantum dots. Specifically, we report electric field-induced modulation of absorption in PbS quantum dots of diameters 5 nm and 7 nm with maxima in the electroabsorption spectra occurring at 1350 nm and 1635 nm, corresponding closely with the positions of the excitonic peaks of the respective unperturbed absorption spectrum.

Optical modulators based on electroabsorption[6] and electro-optic modulation of the refractive index[7] are at the heart of fiberoptic communications networks. These devices convert continuous-wave optical power from a laser source into a stream of intensity- and/or phase-modulated signal variations in order to carry information at high bit rates over thousands of kilometers. Lattice-matched compound semiconductor approaches require multiple selective-area epitaxial growth, etching, and regrowth steps,[6,7] making optoelectronic integration today a costly, low-yield, unscalable technique.

In contrast, solution-synthesized nanoparticles potentially provide a range of functions—emission, detection, modulation, nonlinear optical response—with customization in spectral response and optical functionality achieved through size-effect tuning, organic ligand exchange, and the choice of surrounding matrix material and device structure.

Electroabsorption measurements in ensembles of CdSe and CdS quantum dots across the visible spectral range (500–800 nm) have been used to elucidate the nature of nanocrystal electronic states.[8–11] The observed spectral responses, while similar in size- and field-dependence, have been attributed to a number of different physical mechanisms. Subsequently reported electric field-induced spectral shifts in individual visible light-emitting quantum dots evidence the influence of an external field acting on a dot with a built-in dipole, thereby explicating spectral broadening as the dominant effect in an ensemble of such dots.[12] The physical origins of the built-in dipole observed in CdSe dots have been attributed to either the inherent asymmetry of the wurtzite crystal structure,[13] or the influence of trapped charges on or near the surface of a nanocrystal.[14]

Here we report the measurement of electroabsorption in infrared solution-processed quantum dots. We focus in particular on the spectral electroabsorption behavior of PbS quantum dots (5 nm and 7 nm diameter) over the spectral region 600–2000 nm. The device architecture used herein consists of PbS nanocrystals synthesized via an organometallic method[15] and sandwiched between SiO films. The bottom 360 nm-thick layer of SiO is thermally evaporated onto a glass substrate overcoated with indium tin oxide (ITO), which serves as the bottom electrical contact. Nanocrystal films ~700 nm thick are spin-coated onto the SiO-covered substrate and are then over-coated with a top layer of 150 nm-thick SiO, followed by a 5 nm layer of Au which serves as the top electrical contact.

A 260 Hz sine wave voltage was applied with amplitudes between 25 V and 65 V. Monochromatic light was incident perpendicular to the sample surface and thus parallel to direction of the applied field. The electroabsorption signal reported herein was acquired at twice the frequency of the applied voltage via lock-in detection and from it was determined the change in absorption per unit length.[16] Unmodulated absorption spectra were measured using the Cary 500 spectrophotometer.

Figure 1 shows the unmodulated absorption [Figs. 1(a) and 1(b)], the measured change in absorption due to the modulated applied electric field [Figs. 1(c) and 1(d)], and the calculated second derivative of absorption [Figs. 1(e) and 1(f)] for 5 nm and 7 nm diameter nanocrystals. The insets of Figs. 1(a) and 1(b) show the set of optical transitions revealed in the quantum dots as a result of the electroabsorption spectroscopy provided by these measurements. These

[a]Electronic mail: Ethan.Klem@utoronto.ca

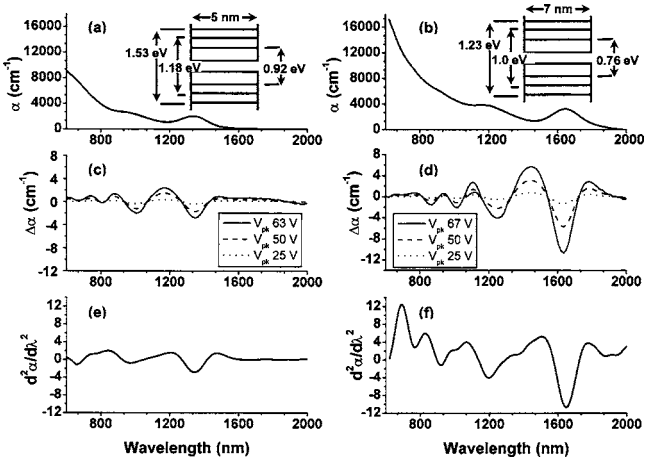

FIG. 1. Unmodulated absorption spectrum (a, b), electroabsorption spectrum (c, d), and second derivative of the linear absorption (e, f) for devices based on 5 nm (a, c, e) and 7 nm (b, d, f) PbS nanocrystals. The insets show the transitions corresponding to first three peaks in the measured electroabsorption spectrum.

transitions correspond to the negative lobes of the electroabsorption spectrum. We show in Fig. 2 the dependence of the amplitude of the measured electroabsorption signal on an applied peak voltage (V_{pk}) at each of the first three optical transitions, revealing a quadratic dependence on field.

We use the framework of Liptay[17] previously employed to determine the change in absorption due to a large applied field in molecules and subsequently used in the study of CdSe nanocrystals[11] to relate observed shifts in absorption spectrum to underlying physical mechanisms. For an ensemble of NCs with distinct separation of energy levels, the change in the absorption spectrum can be expressed as a sum of the zeroth, first, and second derivatives of the unperturbed absorption spectrum.[11] The zeroth order term corresponds to a change in oscillator strength, the first derivative to a shift in energy levels, and the second derivative to a broadening of the absorption spectrum.[18] A comparison of the Stark spectrum to the derivatives of the absorption spectrum provides immediate evidence of the dominant effects of the electric field. As can be seen in Figs. 1(e) and Fig. 1(f), the second derivative fits very well to the first excitonic transition, and the second excitonic transition maps well also. The results suggest that broadening is the dominant effect of the electric field for these transitions.

The mechanism and quantitative features of dipole broadening have been studied in quantum dots resonant with visible wavelengths; we seek to compare these past results with those reported herein for quantum dots resonant in the infrared. Quantitatively, spectral broadening in electroabsorption studies of ensemble samples can be pictured as arising when a collection of randomly oriented dipoles are blue- or redshifted in an applied electric field, depending upon their orientation with regard to field polarity.[18] The change in optical density is predicted to be proportional to[17]

(a) $d^2/d\nu^2(\mathrm{OD}(\nu)/\nu)$, the second derivative of {the optical density spectrum divided by frequency};
(b) F^2, the square of the internal field within the nanocrystals;
(c) $|\Delta\mu|^2$, the square of the magnitude of the change in dipole moment between the initial and final state.

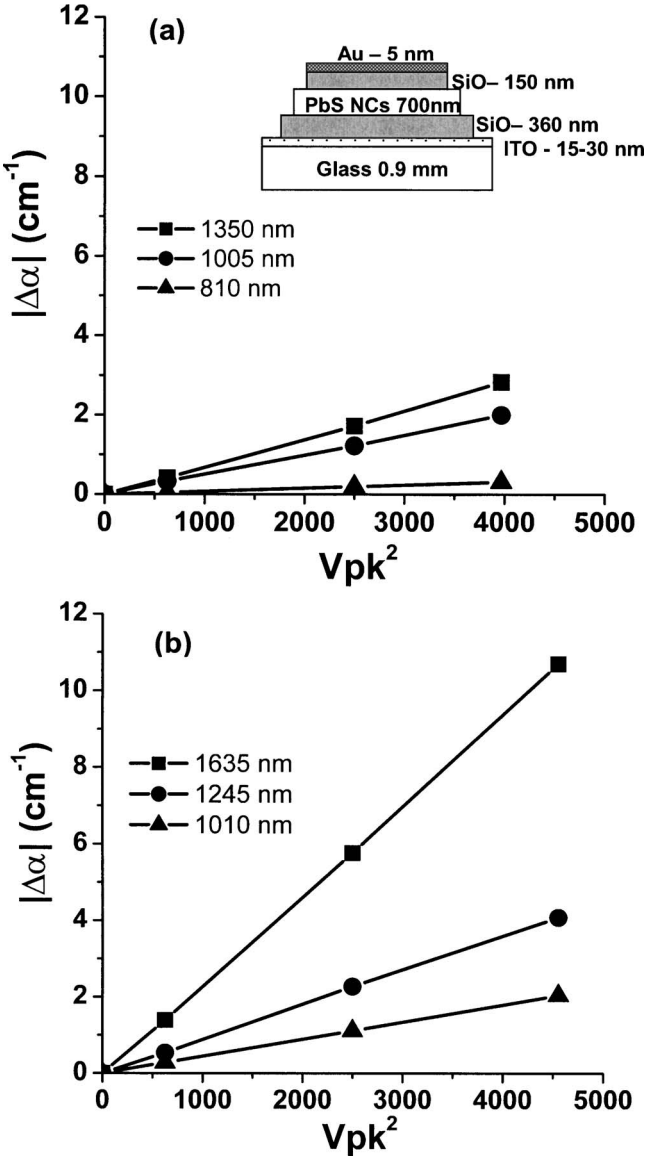

FIG. 2. Change in absorption as a function of the square of applied voltage for the lowest three energy levels for (a) 5 nm nanocrystal device and (b) 7 nm nanocrystal device. A quadratic dependence of $\Delta\alpha$ on V^2 is observed. The inset shows the device structure used for measurements.

The magnitude of the electric field inside the quantum dots is estimated from the external applied field by dividing across the SiO insulating layers and the ligand-capped nanocrystals. For our structure, approximately half of the externally applied field appears across the dots themselves. We used the measured absorption spectrum, modulation spectrum, and estimate of field to estimate the change in dipole moment associated with the first excitonic transition. For 5 nm nanocrystals we found $\Delta\mu=13\pm1$ D and for 7 nm $\Delta\mu=17\pm0.5$ D. These changes in dipole moments are smaller than that observed in CdSe where, for nanocrystals ranging in size from 2 to 5 nm, $\Delta\mu$ varied from 20 to 100 D.[11]

In CdSe nanocrystals the dipole moment has been attributed to the lack of inversion symmetry inherent in its wurtzite crystal structure,[19] although in Ref. 14 the influence of trapped charges is thought to dominate over the crystalline structure. PbS, however, has a rock salt crystal structure with cubic symmetry; we therefore propose that the excited state

dipole arises not from a crystal asymmetry but from a coupling of the interior carrier wave functions to surface states associated with unpassivated dangling bonds.[11,12] This picture is supported by single-nanocrystal studies of the spectral shift in the photoluminescence (PL) of CdSe dots under the influence of an applied electric field which have shown the presence of trapped charge on or near the surface of the nanocrystal contributes to the observed polar component of the excited state.[12] Although the spectral shift of a single nanocrystal has both linear and quadratic components under the influence of an electric field, an average over multiple dots results in a purely quadratic broadening effect similar to that found here.

The observed magnitude of $\Delta\mu$ for comparable sizes of PbS and CdSe dots is influenced by a number of factors, including the relative dielectric constants ($\varepsilon_r=17$ for bulk PbS, $\varepsilon_r=10.6$ for bulk CdSe), and the number of available surface and defect states available.[14] Comparison of $\Delta\mu$ between samples and sample structures is complicated by the treatment of the applied field in the presence of the surrounding medium.[18] However a comparison of observed magnitudes of $\Delta\mu$ between similar sized CdSe and PbS nanocrystals shows nearly an order of magnitude greater change in the case of CdSe. A factor contributing to this difference is the density of surface states: CdSe, with its wurtzite structure, may possess as many as three dangling bonds per surface atom,[13] whereas PbS, with its cubic rock-salt structure, has a single dangling bond per surface atom. The combination of the differences between the dielectric constants, the density of surface states, and the crystal structure account for differences in the measured $\Delta\mu$ here and CdSe measured previously.

The reduction in $\Delta\mu$ for the smaller sized PbS particles can be attributed to the decrease in nanocrystal volume. The net distance over which charges can be separated within the nanocrystal decreases as a result of the decrease in size. Furthermore, the field strength in the interior of the nanocrystal from a trapped surface charge will be larger for smaller dots, leading to an increased screening of the applied field. This result is consistent with the trends observed in CdSe and ZnS nanocrystals.[12,14]

The change in the real part of the refractive index (Δn) was estimated through the Kramers-Kronig relations.[16] The 5 nm nanocrystals exhibit a peak Δn of 10^{-5} at 1280 nm and beyond the band-edge have a peak Δn of 6×10^{-6} at 1430 nm. The 7 nm nanocrystals have a peak Δn of 2×10^{-5} at 1550 nm and 1.5×10^{-5} at 1725 nm. These results are an order of magnitude higher than that obtained from $CdS_{0.44}Se_{0.56}$ quantum dots.[16] For this material to be useful for practical modulator applications it is necessary to compare the strength of the observed electro-optic effect to those of traditional material systems such as GaAs and $LiNbO_3$.[20] Using the expression $\Delta n=\frac{1}{2}rn_0^3E$, where r is the linear electro-optic coefficient, n_0 is the material refractive index, which we estimate to be 1.8–1.9 through transmission measurements and spacing of Fabry-Perot peaks in PbS films, and E is the strength of the applied field seen by the nanocrystals, we calculate $r\sim0.39$ pm/V for our 7 nm nanocrystals at 1550 nm and $r\sim0.29$ pm/V at 1725 nm. These numbers compare to $r_{33}=30.8$ pm/V for $LiNbO_3$ and $r_{41}=1.4$ pm/V for GaAs.[20] Though the calculated coefficients for solution-processed PbS nanocrystals are lower than $LiNbO_3$ and GaAs they are expected to be polarization independent due to the isotropic nature of the ensemble of randomly oriented dipoles.

This evidence of electroabsorption in PbS nanocrystals motivates future work directly measuring the electro-optic effect, particularly since calculated changes in the real part of the index of refraction occur beyond the absorption edge of the nanocrystals. This phenomenon may potentially be exploited to create a modulator based on phase-shifted interference. The use of nanocrystals processed by spin-casting out of solution allows this device to be integrated onto a variety of substrates, including silicon, in a CMOS-compatible process.

[1]"Electronic & Photonic Integrated Circuit (EPIC)," Announcement BAA04-15, Defense Advanced Research Projects Agency, Arlington, VA (2004).
[2]N. Tessler, V. Medvedev, M. Kazes, S.-H. Kan, and U. Banin, Science **295**, 1506 (2002).
[3]E. H. Sargent, Adv. Mater. (Weinheim, Ger.) **17**, 515 (2005).
[4]J. Steckel, S. Coe-Sullivan, V. Bulovic, and M. G. Bawendi, Adv. Mater. (Weinheim, Ger.) **15**, 1862 (2003).
[5]R. D. Schaller, M. A. Petruska, and V. I. Klimov, J. Phys. Chem. B **107**, 13765 (2003).
[6]B. Mason, A. Ougazzaden, C. W. Lentz, K. G. Glogovsky, C. L. Reynolds, G. J. Przybylek, R. E. Leibenguth, T. L. Kercher, J. W. Boardman, M. T. Rader, J. M. Geary, F. S. Walters, L. J. Peticolas, J. M. Freund, S. N. G. Chu, A. Sirenko, R. J. Jurchenko, M. S. Hybertsen, L. J. P. Ketelsen, and G. Raybon, IEEE Photonics Technol. Lett. **14**, 27 (2002).
[7]C. Lawetz, J. C. Cartledge, C. Rolland, and J. Yu, J. Lightwave Technol. **15**, 697 (1997).
[8]A. Ekimov, A. Efros, T. Shubina, and A. Skvotsov, J. Lumin. **46**, 97 (1990).
[9]S. Nomura and T. Kobayashi, Solid State Commun. **73**, 425 (1990).
[10]D. Cotter, H. Girdlestone, and K. Moulding, Appl. Phys. Lett. **58**, 455 (1991).
[11]V. Colvin, K. Cunningham, and A. Alivisatos, J. Chem. Phys. **101**, 7122 (1994).
[12]S. A. Empedocles and M. G. Bawendi, Science **278**, 2114 (1997).
[13]E. Rabani, B. Hetenyi, B. J. Berne, and L. E. Brus, J. Phys. Chem. **110**, 5355 (1999).
[14]M. Shim and P. Guyot-Sionnest, J. Chem. Phys. **111**, 6955 (1999).
[15]M. A. Hines and G. D. Scholes, Adv. Mater. (Weinheim, Ger.) **15**, 1844 (2003).
[16]K. Stokes and P. Persans, Phys. Rev. B **54**, 1892 (1996).
[17]W. Liptay, *Advances in Electronic Excitation and Relaxation*, edited by E. C. Lim (Academic, New York, 1974), p. 129.
[18]G. Bublitz and S. Boxer, Annu. Rev. Phys. Chem. **48**, 213 (1997).
[19]L. Li and A. P. Alivisatos, Phys. Rev. Lett. **90**, 7402 (2003).
[20]G. L. Li and P. K. L. Yu, J. Lightwave Technol. **21**, 2010 (2003).